Vol. 78, No. 3

Fibrinogen Regulates the Cytotoxicity of Mycobacterial Trehalose Dimycolate but Is Not Required for Cell Recruitment, Cytokine Response, or Control of Mycobacterial Infection[∇]

Kaori Sakamoto,[1]* Rachel E. Geisel,[2] Mi-Jeong Kim,[2] Bryce T. Wyatt,[1] Llewelyn B. Sellers,[1] Stephen T. Smiley,[3] Andrea M. Cooper,[3] David G. Russell,[2] and Elizabeth R. Rhoades[4]

Department of Pathology, College of Veterinary Medicine, 501 D.W. Brooks Dr., University of Georgia, Athens, Georgia 30602-7388[1]; Department of Microbiology and Immunology, Cornell University Veterinary Medical Center, Ithaca, New York 14853[2]; Trudeau Institute, Saranac Lake, New York 12893[3]; and Cornell Nanoscale Science and Technology Facility, 250 Duffield Hall, Cornell University, Ithaca, New York 14853[4]

During inflammatory responses and wound healing, the conversion of soluble fibrinogen to fibrin, an insoluble extracellular matrix, long has been assumed to create a scaffold for the migration of leukocytes and fibroblasts. Previous studies concluded that fibrinogen is a necessary cofactor for mycobacterial trehalose 6,6′-dimycolate-induced responses, because trehalose dimycolate-coated beads, to which fibrinogen was adsorbed, were more inflammatory than those to which other plasma proteins were adsorbed. Herein, we investigate roles for fibrin(ogen) in an *in vivo* model of mycobacterial granuloma formation and in infection with *Mycobacterium tuberculosis*, the causative agent of tuberculosis. In wild-type mice, the subcutaneous injection of trehalose dimycolate-coated polystyrene microspheres, suspended within Matrigel, elicited a pyogranulomatous response during the course of 12 days. In fibrinogen-deficient mice, neutrophils were recruited but a more suppurative lesion developed, with the marked degradation and disintegration of the matrix. Compared to that in wild-type mice, the early formation of granulation tissue in fibrinogen-deficient mice was edematous, hypocellular, and disorganized. These deficiencies were complemented by the addition of exogenous fibrinogen. The absence of fibrinogen had no effect on cell recruitment or cytokine production in response to trehalose dimycolate, nor was there a difference in lung histopathology or overall bacterial burden in mice infected with *Mycobacterium tuberculosis*. In this model, fibrin(ogen) was not required for cell recruitment, cytokine response, or response to infection, but it promoted granulation tissue formation and suppressed leukocyte necrosis.

Fibrinogen is an approximately 340-kDa circulating glycoprotein, a heterotrimer of Aα, Bβ, and γ chains (35). This plasma protein is produced primarily in the liver by hepatocytes, with strong upregulation in response to proinflammatory agents (16, 20, 35). The role of fibrinogen in the coagulation cascade is well characterized, with the cleavage of fibrinogen by thrombin to form fibrin, which then is covalently cross-linked by activated Factor XIII to form the rigid, hemostatic fibrin clot. Less well-known are the other functions of fibrin(ogen), such as the mediation of platelet spreading, the promotion of angiogenesis, and the stimulation of fibroblast proliferation (3, 7, 14, 22, 34). Fibrin(ogen) also is thought to provide a scaffold along which leukocytes can migrate, and stimulated monocytes and neutrophils express a high-affinity receptor for fibrin(ogen), the integrin $\alpha_M\beta_2$ (Mac-1) (1).

Mycobacterium tuberculosis is the leading cause of death due to bacterial infection and currently is estimated to infect a third of the world population (10, 12). In the context of tuberculosis, fibrinogen has been shown to be upregulated during experimental tuberculosis in mouse models and in natural human

infections, as occurs in other infectious diseases, resulting in a hypercoagulable state (15, 30). Fibrinogen also has been identified as a cofactor for the pathological effects of mycobacterial trehalose 6,6′-dimycolate (TDM). Retzinger et al. demonstrated that TDM adsorbed fibrinogen preferentially to the exclusion of other plasma proteins, which increased the pyogranulomatous response to TDM (25). TDM is a predominant mycobacterial cell wall component and an important virulence factor for *M. tuberculosis*, in that it is granulomagenic, can delay phagosome maturation, and is an active component of complete Freund's Adjuvant (2, 17, 18, 32). The presentation of TDM as a higher-order polymer, as a monolayer either in oil-water emulsions or on polystyrene particles, is required for maximal bioactivity (13, 26). We use a bead-based delivery model using 90-μm polystyrene microspheres suspended within Matrigel, a commercially available mixture of extracellular matrix components, to study the contributions of individual lipids to the inflammatory response to mycobacteria (13, 27).

The development of a fibrinogen Aα chain-deficient mouse (Fib knockout [KO]) has facilitated the direct study of the roles of fibrinogen in inflammation (36). The use of this mouse strain has revealed the roles of fibrinogen in the limitation of *Listeria monocytogenes* growth *in vivo* (21), in the exacerbation of crescentic glomerulonephritis (9), in the organization of wound healing and wound stability (8), in tumor metastasis (23), and in cell adhesion to biomaterials (6). On the other

hand, a study of bleomycin-induced pulmonary fibrosis in Fib KO mice showed that fibrosis developed independently of fibrin(ogen), and the absence of fibrin(ogen) increased the presence of neutrophils (40).

In this study, we use a subcutaneous granuloma model in Fib KO mice to determine whether fibrinogen is necessary for the inflammatory response to TDM. Our results show that while fibrinogen is important for the organized formation of granulation tissue, fibrinogen deficiency has no effect on leukocyte recruitment to TDM-coated beads or proinflammatory cytokine production by the recruited cells. Fib KO mice also show no differences in pulmonary histopathology and only a transient difference in pulmonary bacterial burden in response to intravenous infection with *M. tuberculosis*. However, Fib KO mice show a suppurative response to TDM, resulting from the exacerbation of neutrophil necrosis and matrix degradation, whereas wild-type (WT) mice develop a granulomatous response with less cell degeneration, necrosis, and matrix degradation. These results show that fibrinogen is required neither as a cofactor for initiating an inflammatory response to TDM nor for controlling infection with *M. tuberculosis*, but rather suppresses the cytotoxic effects of TDM on recruited neutrophils while promoting the formation of granulation tissue.

MATERIALS AND METHODS

Mice and cell culture. Fib KO mice (36) that were backcrossed seven generations to C57BL/6 mice were generously supplied by Jay Degen (Children's Hospital Research Foundation, Cincinnati, OH) and were bred at the Cornell University Transgenic Mouse Core Facility. Tail snip genotyping was used to identify the Fib KO, heterozygous (HET), and WT mice. Two- to 7-month-old male and female mice were used for all *in vivo* experiments with the randomization of age and the sex of individuals within and between treatment groups. Mice were weighed immediately after injection and every other day thereafter. Animals were housed in a specific-pathogen-free animal facility. The Cornell University Institutional Animal Care and Use Committee reviewed and approved all techniques used in these experiments. Murine bone marrow-derived macrophages (BMMΦ) were cultured as described previously (13).

Neutrophils were harvested from WT bone marrow using fluorescein isothiocyanate (FITC)-labeled, anti-mouse Gr-1/Ly-6G antibody (1A8; BD Biosciences, San Jose, CA) and anti-FITC magnetic beads (Miltenyi Biotec, Gladbach, Germany), followed by positive selection using an LS magnetic column in a Midi MACS separation system (Miltenyi) by following the manufacturer's protocol, with slight modifications. Gr-1-positive macrophages were removed by adherence to bacteriologic-grade 90-mm² petri dishes (Kord-Valmark). Nonspecific antibody binding was prevented by incubation with anti-mouse FcγIII/IIR (5 μg/ml; 2.4G2; Caltag Laboratories, Burlingame, CA) antibody in 0.5% bovine serum albumin (BSA)–phosphate-buffered saline (PBS). Degassed 0.5% bovine serum albumin (Sigma-Aldrich, St. Louis, MO) in PBS and sterile PBS were used as running and rinsing buffers, respectively. All medium components were free of endotoxin as determined by using the *Limulus* amoebocyte lysate assay (Cambrex, Charles City, IA).

Trehalose dimycolate. TDM was purified from *Mycobacterium bovis* Bacille Calmette-Guérin (BCG) as described previously (13). Stocks were stored in chloroform-methanol (2:1, vol/vol) under nitrogen gas at −20°C. *M. tuberculosis* strain H37Rv TDM, purchased from Sigma-Aldrich, was diluted in *n*-hexane and used for the *in vitro* neutrophil experiments.

Subcutaneous granuloma model. TDM was coated onto the surface of 90-μm polystyrene microspheres (Polysciences, Inc., Warrington, PA) as previously described (27). Approximately 2×10^3 TDM-coated beads and 10^7 BMMΦ of the appropriate genotype were added per ml of an ice-cold solution of growth factor-reduced Matrigel (90% in PBS; BD Biosciences). Three hundred microliters of this mixture was injected subcutaneously in the scruff. Fibrinogen was not detected in the Matrigel using an immunoblot technique with biotin-labeled rabbit anti-mouse fibrinogen IgG (Molecular Innovations, Novi, MI). All granuloma components and exogenous fibrinogen (Sigma-Aldrich) were tested routinely for endotoxin by the *Limulus* amoebocyte assay. Please note that since 2007, Polysciences has changed the formulation of its polystyrene particles,

altering the hydrophobicity and therefore the capacity of lipid coating. Similar results have been achieved, however, using hydrophobic polystyrene particles with a mean diameter of 80 μm from Duke Scientific (Fremont, CA).

***In vitro* neutrophil experiments.** TDM was dissolved in *n*-hexane by sonication at 56°C. Twenty-four-well plates were coated with 5 μg/well of TDM in *n*-hexane or *n*-hexane only and dried overnight. Neutrophils were harvested as described above and then added to TDM-treated, *n*-hexane-treated, or untreated wells at 1×10^5 cells per well, and then untreated cells were stimulated with 60 μM staurosporine (Sigma). Cells were treated in the presence or absence of 250 μg of murine fibrinogen (Sigma) per well in a final volume of 500 μl. Neutrophils were stimulated for 2 h at 37°C and 5% CO_2, stained using allophycocyanin (APC)-annexin V (Invitrogen) and propidium iodide (PI; 10 μl/200 μl; BD Biosciences) by following manufacturer protocols, and then analyzed by flow cytometry using a two-laser, four-color FACSCalibur and collecting at least 20,000 events. Antibodies against F4/80, CD3ε (145-2C11), CD19 (1D3), major histocompatibility complex class II (MHC-II) (2G9), and Gr-1/Ly-6G (1A8) were used as described below to determine neutrophil purity, which routinely was 70 to 80%. Contaminating cells were determined by flow cytometry to be Gr-1-positive macrophages or bead-labeled cell fragments. Percentages of necrotic or apoptotic neutrophils were determined first by gating upon FITC-positive cells, followed by the analysis of the percentages of PI-positive and APC-annexin V-positive cells.

Flow cytometry. Cells were recovered from matrices and processed as described previously (27). Cells were incubated in fluorescent-activated cell sorting (FACS) buffer containing fluorophore-conjugated antibodies from Caltag, BD Pharmingen, or eBioscience (San Diego, CA) for 45 min. Antibodies were used at 0.5 to 2 μg/ml except for MHC-II (2G9), which was used at 5 μg/ml. Other antibodies used were Gr-1 (Ly-6G and Ly-6C, RB6-8C5), F4/80, CD3ε (145-2C11), CD4 (CT-CD4), CD8α (53-6.7), CD19 (1D3), CD25 (PC61), CD45 (30-F11), pan-NK (DX5), and γδ-TCR (GL3). Propidium iodide (10 μl/200 μl; BD Biosciences) was added during the last 10 min of staining. Cells positive for propidium iodide were gated out prior to collecting at least 10,000 events.

Leukocyte subsets were identified using the following cytometric parameters on a two-laser, four-color FACSCalibur using CellQuest software (BD Biosciences): neutrophils (side scatter [SSC]^{lo}, Gr-1^{mid}, or Gr-1^{hi}, and MHC-II$^-$ F4/80$^-$), macrophages (Gr-1^{hi} or Gr-1^{mid}, and MHC-II$^+$ F4/80$^+$), eosinophils (SSC^{mid} Gr-1^{mid} MHC-II$^-$ F4/80^{mid}), B cells (SSC^{lo} CD19$^+$), CD4 T cells (SSC^{lo} CD3$^+$ CD4$^+$), CD8 T cells (SSC^{lo} CD3$^+$ CD8$^+$), NK cells (SSC^{lo} pan$^-$ NK$^+$), and γδ T cells (SSC^{lo} CD3$^+$ γδ TCR$^+$). Cell numbers were determined for each mouse in each group ($n = 4$ or 5) by multiplying subset percentages by the number of trypan blue-negative (viable) cells and normalizing to the weight of the matrix from which the cells were retrieved.

ELISA. A portion (between 20 and 30 mg) of each harvested matrix was cultured for 48 h in 500 μl of Dulbecco's modified essential medium (DMEM) supplemented with 10% heat-inactivated fetal calf serum, 2 mM L-glutamine, 1 mM sodium pyruvate, 100 U/ml penicillin, and 100 μg/ml streptomycin. Supernatants were collected, centrifuged to remove granuloma pieces, and stored at −80°C. Sandwich enzyme-linked immunosorbent assays (ELISAs) for tumor necrosis factor-α (TNF-α), interleukin-6 (IL-6), IL-1α, and IL-1β were performed according to the manufacturer's instructions (BD Biosciences).

Histology, immunohistochemistry, and immunofluorescence. A portion of representative matrices was fixed immediately in 4% paraformaldehyde in PBS for at least 24 h at 4°C, followed by transfer to 70% ethanol for at least 24 h before submission for processing and sectioning by the Cornell University College of Veterinary Medicine Histology Laboratory. Briefly, samples were embedded in paraffin, sectioned at 4 μm thickness, and stained with either hematoxylin and eosin (H&E) or Masson's trichrome stain.

For caspase 3 detection, sections of 7-day-old TDM matrices from Fib KO mice were incubated in 0.01 M citrate buffer, pH 6.0, in a microwave for two 10-min intervals at 800 W for antigen retrieval and then incubated for 2 h at 37°C with rabbit anti-caspase 3 diluted 1:50 in PBS–1× casein. Biotinylated goat anti-rabbit IgG H+L (Vector, Burlingame CA) was applied for 20 min at room temperature, and slides were washed and incubated for 20 min with streptavidin peroxidase (Zymed). AEC substrate was prepared as directed (Zymed kit) and applied for 10 min. Slides were counterstained with Gill's #2 hematoxylin and mounted with Fluoromount G (both from Fisher Scientific, Fremont, CA). Negative controls were included, substituting normal rabbit IgG (Vector) for the primary antibody at the appropriate dilution equal to the final concentration (μg/ml) of primary antibody.

For immunofluorescence, sections of 7-day-old TDM matrices from Fib KO mice were incubated in 1:50 dilutions of rabbit anti-human neutrophil elastase (Fitzgerald Industries, Inc., Concord, MA) and mouse anti-human histone H1 (Acris Antibodies, Herford, Germany) or no primary antibody (negative control)
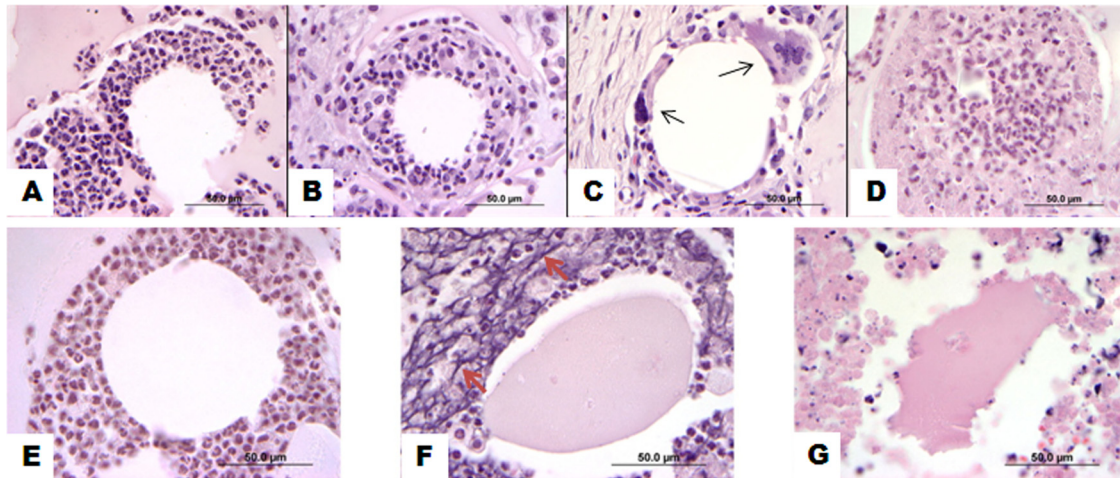
FIG. 1. Subcutaneous TDM matrices in WT mice are primarily neutrophilic at early time points but later become pyogranulomatous to granulomatous, while Fib KO matrices become progressively suppurative. WT and Fib KO mice ($n = 4$ to 5 per time point) were injected subcutaneously in the scruff with 300 μl of TDM-coated 90-μm-diameter microspheres suspended within Matrigel. Matrices were removed for analysis at days 4 (A and E), 7 (B and F), and 12 (C, D, and G). Representative samples were fixed, sectioned, and stained with H&E. Photomicrographs represent leukocytic infiltrates in WT matrices (A to D) and in Fib KO matrices (E to G) typical for the depicted time point and are representative of three separate experiments. Multinucleated giant cells (black arrows) are present in panel C. An area showing neutrophil degeneration and necrosis, as well as peripheral eosinophilic ghost cells, as observed sporadically in 12-day-old TDM matrices from WT mice, is shown in panel D. The nuclear streaming of recruited neutrophils (red arrows) is prominent in panel F. Original magnification, ×1,000; bar = 50 μm.

overnight at 4°C, and then they were wetted with 1:1,000 Draq5 (Biostatus Ltd., Leicestershire, United Kingdom) immediately before being mounted in 9% Mowiol 4-88 (Calbiochem, La Jolla, CA) in glycerol-Tris (1:4, vol/vol). Confocal microscopy was performed using an AxioImager M1 microscope with a laser-scanning microscope (LSM) 510 Meta confocal head with an EC PLAN Neofluor (×40 magnification, 1.3 numeric aperture) oil lens and Argon2 and HeNe lasers (Carl Zeiss, Jena, Germany). Images were created using LSM 510 version 4.0 SP2 (Carl Zeiss MicroImaging GmbH). Images were processed using Adobe Photoshop CS2 version 9.0.2 (Adobe Systems Inc., San Jose, CA). Autocontrast tools were used on all of the images equally.

***M. tuberculosis* intravenous infection model.** Two-month old, female Fib KO and HET mice that were bred and maintained at the Trudeau Institute were used for this experiment. *M. tuberculosis* strain H37Rv was grown as previously described (29). Mice were injected intravenously via the tail vein at a final dose per mouse of 1×10^5 CFU in saline. Mice were euthanized by CO_2 narcosis, and samples of lung, spleen, and liver then were individually homogenized in physiological saline, and serial dilutions of the organ homogenate were plated on nutrient 7H11 agar. Bacterial CFU were counted after 3 weeks of incubation at 37°C (29). A caudal lung lobe was perfused with 10% formalin–saline and fixed for 1 week. Tissues were sent to Colorado Histoprep (Fort Collins, CO) for routine paraffin embedding, serial sectioning, and staining using H&E and acid-fast stains.

Statistical methods. All cell number calculations and cytokine measurements were performed for individual mice, and the standard deviations (SD) from the mean values ($n = 4$ or 5) are presented. The statistical significance of differences in the means between Fib KO and HET or WT mice was calculated using a Student's t test.

RESULTS

The response to BCG TDM in the subcutaneous compartment of WT mice is pyogranulomatous, as opposed to suppurative, in Fib KO mice. Previously, we developed a peritoneal granuloma model to study the immunostimulatory activity of different mycobacterial lipids (13). In preliminary experiments, the injection of TDM matrices into the peritoneal cavity of Fib KO mice resulted in fragmented pieces instead of the cohesive, adherent matrices typically observed in our peritoneal granuloma model in WT mice (13 and data not shown). As the increased exposed surface area of TDM-bearing matrix could skew cell recruitment to the matrices, we opted for subcutaneous injection, wherein the matrices would be trapped as a single mass in the subcutis.

By histologic examination, neutrophils were the primary leukocyte recruited to the TDM beads in WT mice at 4 and 7 days, with a shift toward increasing numbers of macrophages beginning at 7 days and then a predominant macrophage response at 12 days, with occasional multinucleated giant cells (Fig. 1A to C). By day 12, scattered foci within, but not limited to, the center of the granulomas also contained eosinophilic ghost cells of recruited neutrophils and macrophages, accompanied by the degradation of the matrix, resembling early features of caseous necrosis (Fig. 1D). These histologic features, an early neutrophilic response developing into pyogranulomatous inflammation, are similar to those reported in our peritoneal granuloma model (13), differing only in slower kinetics.

At 4 days, the beads in granulomas from Fib KO mice were cuffed by moderate numbers of neutrophils, similarly to those in the WT and HET mice (Fig. 1E). By day 7, however, severe neutrophilic infiltration, with the degeneration and necrosis of these leukocytes and nuclear streaming, was the predominant feature in these matrices (Fig. 1F). These features were accompanied by the degradation of the Matrigel, characterized by the contraction of the fractured pieces and hypereosinophilic staining. At day 12, the centers of some of these matrices were completely degraded and difficult to examine histologically, as much of the liquefied material was washed away during processing (Fig. 1G). The increased liquefactive necrosis and destruction of the matrix observed in Fib KO mice shows that fibrinogen suppresses the cytotoxic effects of TDM or improves the survival of neutrophils in this subcutaneous model.

Fibrinogen is required for early organized granulation tissue formation, and this deficiency can be complemented by
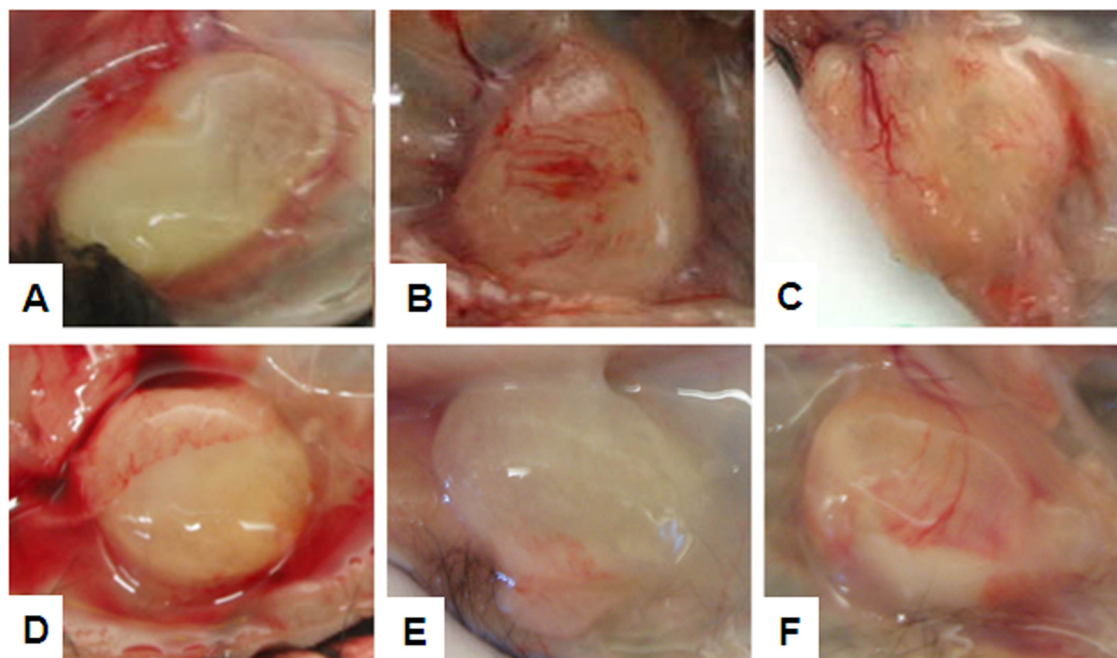
FIG. 2. Subcutaneous TDM matrices in Fib KO are grossly similar to those of the WT, with slight delays in neovascularization. TDM matrices from WT (A to C) and Fib KO (D to F) mice were removed at days 4 (A and D), 7 (B and E), and 12 (C and F).

exogenous fibrinogen. In WT and HET mice, adherent, neovascularized, pale yellow-white, translucent granulomas formed by day 4 and developed a pale pink capsule by day 12 (Fig. 2A to C and data not shown). Matrices injected into Fib KO mice also were pale yellow and adherent to the surrounding tissues; however, at days 4 and 7, they generally were less vascularized than those in WT mice (Fig. 2D and E). By day 12, however, the matrices in Fib KO mice were covered by a pale pink, well-vascularized capsule, grossly indistinguishable from those in the WT or HET mice (Fig. 2F). In contrast to the WT and HET mouse granulomas, the centers of KO granulomas occasionally were white, liquefied, and oozed from the cut surface.

The histologic examination of the periphery of 4-day-old TDM matrices in WT or Fib KO mice revealed loosely arranged but parallel fibroblasts interspersed with neutrophils and macrophages (Fig. 3A and D). Well-developed granulation tissue was present around the WT matrices by day 7, with the characteristic parallel sheets of fibroblasts perpendicularly transected by immature blood vessels and interspersed with neutrophils, macrophages, and lymphocytes (Fig. 3B). By day 12, mature collagen could be observed surrounding granulomas from these mice (Fig. 3C). Fib KO mice, on the other hand, did not develop well-organized granulation tissue until day 12. Tissues surrounding 7-day-old matrices instead were edematous, hypocellular, and poorly vascularized (Fig. 3E). This delay in the development of granulation tissue in Fib KO mice at 7 days was complemented by the addition of 500 μg/ml of fibrinogen (Sigma) to the matrix prior to injection (Fig. 3F). This dose of exogenous fibrinogen was selected because it was the highest circulating concentration of fibrinogen reported during experimental *Candida* peritonitis in mice (28) and was the highest dose that could be added to the matrix without diluting it significantly. These results show that fibrinogen aids the early formation of granulation tissue but is not required for capsule formation. Interestingly, the addition of fibrinogen did not reduce the recruited leukocyte death in Fib KO matrices, as determined qualitatively by histopathology (data not shown).

Fibrinogen protects neutrophils from TDM-induced necrosis *in vitro*. To determine the mechanism of cell death induced by TDM in Fib KO mice, and because fibrinogen has been reported previously to delay apoptosis (31), sections of 7-day-old TDM matrices from Fib KO mice were stained for activated caspase 3, an effector caspase in the apoptosis pathway. No staining above that of negative controls was observed (data not shown), supporting the histopathologic evidence that apoptosis was not the mechanism by which recruited neutrophils were dying. We therefore proceeded to study this mechanism *in vitro*, using neutrophils harvested from murine bone marrow. Purified neutrophils were exposed to wells coated with TDM, vehicle control (*n*-hexane), or 60 μM staurosporine for 1, 2, 5, and 18 h in the presence or absence of 500 μg/ml fibrinogen, and then they were stained with APC-annexin V and propidium iodide (PI) to determine the percentages of cells that were apoptotic or necrotic, respectively, by flow cytometry (Fig. 4 and data not shown). Although induced necrosis overall was low, statistical analysis showed significantly greater necrosis ($P < 0.05$) in response to TDM-coated wells at 2 h in the absence of fibrinogen (Fig. 4A). *n*-hexane-coated wells did induce a background level of necrosis; however, it was significantly less ($P < 0.05$) than that induced by TDM (Fig. 4A). Fibrinogen also was significantly protective against necrosis in the *n*-hexane-treated neutrophils. TDM induced negligible neutrophil apoptosis at all of the time points studied (data not shown). Fibrinogen also was protective in decreasing staurosporine-induced apoptosis in neutrophils at 2 h (Fig. 4B), as has been reported previously (31). Fibrinogen, therefore, plays
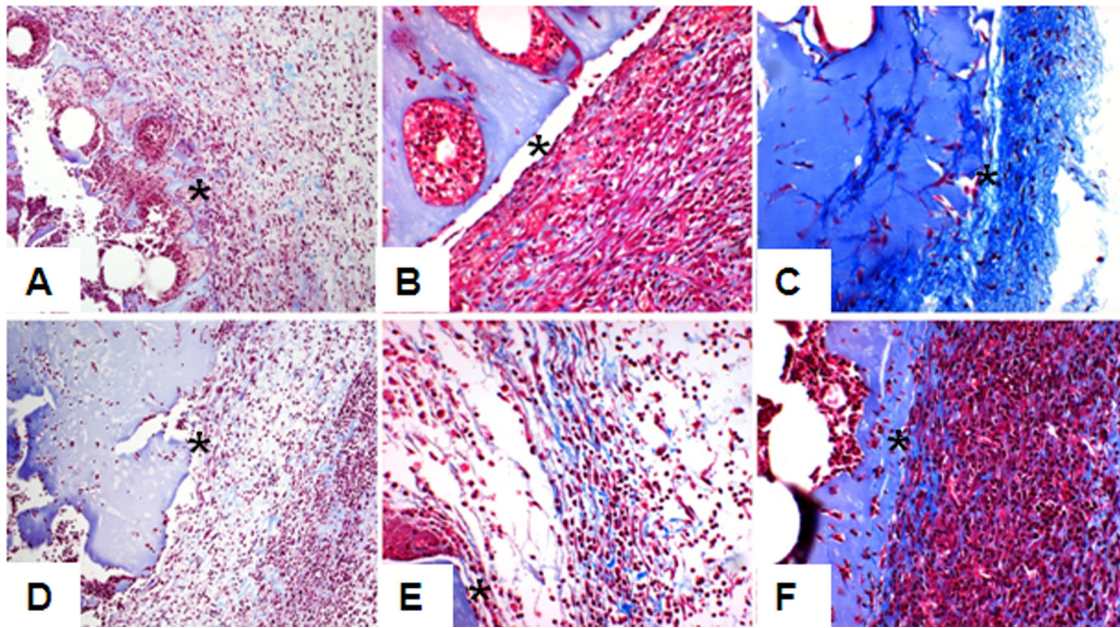
FIG. 3. Granulation tissue and capsule formation in KO matrices is delayed and impaired but can be complemented by the addition of exogenous fibrinogen. Sections of TDM matrices were stained using Masson's trichrome stain to show the deposition of collagen (blue) during capsule formation. The capsule surrounding WT (A) and Fib KO (D) matrices at 4 days is loosely organized and histologically similar. Well-developed granulation tissue surrounds 7-day-old WT matrices (B), and by 12 days (C), the capsule is composed primarily of collagen. (E) In Fib KO matrices, however, the granulation tissue response at 7 days is disorganized, edematous, and hypocellular, similar to the appearance at 4 days. (F) The addition of 500 μg/ml fibrinogen to the KO matrices allows well-organized granulation tissue to surround the matrix at 7 days. Asterisks indicate the interface between Matrigel and capsule. Original magnification, ×200.

a protective role in the preservation of TDM-stimulated neutrophils.

Neutrophil NETs are induced by TDM in the absence of fibrinogen. The nuclear streaming that was a predominant feature of the 7-day-old TDM matrices in Fib KO mice was histologically similar to reports of neutrophil extracellular traps (NETs), which are extruded neutrophil DNA and histones complexed with neutrophil elastases that together have antibacterial activity (4). Furthermore, *M. tuberculosis* recently has been reported to induce NET formation *in vitro* (24). To investigate the possibility that this lesion was consistent with neutrophil NETs and that TDM could be a mycobacterial factor inducing this response, we performed immunofluorescence on sections of Fib KO matrices using anti-neutrophil elastase, anti-histone H1 antibodies, and the DNA stain Draq5 and examined them for colocalization by confocal microscopy. Strong Draq5 and anti-histone H1 staining of the streaming material confirmed the presence of DNA and histone H1 (Fig. 5A and E), while elastase was present both associated with this DNA as well as in the cytoplasm of surrounding intact neutrophils (Fig. 5C). These results suggest that TDM is stimulating the formation of NETs, particularly in the absence of fibrinogen, and that fibrinogen plays a role in the regulation of NETs.

Fibrinogen is not required for cell recruitment or cytokine response to TDM, or for responses to infection with *M. tuberculosis*. The flow-cytometric analysis of cells harvested from granulomas in three separate experiments showed no differences in the number of leukocytes in matrices from WT or HET mice compared to those from Fib KO mice (data not

shown). Leukocytes that were analyzed included neutrophils, macrophages, B cells, T cells (CD4$^+$, CD8$^+$, and γδTCR subsets), and eosinophils that were identified by the combinations of surface markers outlined in Materials and Methods (data not shown). Matrices supplemented with exogenous fibrinogen showed no differences in cell recruitment compared to that of unsupplemented matrices from Fib KO mice (data not shown). Levels of proinflammatory cytokines (TNF-α, IL-6, IL-1α, and IL-1β) were measured in supernatants of cells cultured from explanted matrices. ELISA results showed no consistently significant differences in the cytokines analyzed between the WT and HET groups or the Fib KO group at any of the time points (data not shown). These data suggest that the cell recruitment and cytokine responses to TDM are not dependent upon the presence of fibrinogen.

To test the overall importance of fibrinogen in the context of *M. tuberculosis* infection, Fib KO and HET mice were infected by tail vein injection, and tissues were taken at days 1, 8, 17, 30, and 60 for histopathology and bacterial enumeration. No histopathologic differences were observed in the lung, liver, or spleen at any of the time points (data not shown). A single statistically significant ($P < 0.05$) difference in the load of viable bacteria was observed at 17 days in the lung, with lower numbers in the Fib KO mice (3.57 log$_{10}$ CFU ± 0.05 for Fib KO mice and 3.89 log$_{10}$ CFU ± 0.19 for HET mice) (Table 1). A low-dose (100 CFU) aerosol infection experiment also was performed as described in Mogues et al., and no significant differences in CFU or histopathology were observed at 50 days postinfection (R. North, personal communication) (19). These results suggest that fibrinogen is required for neither immune
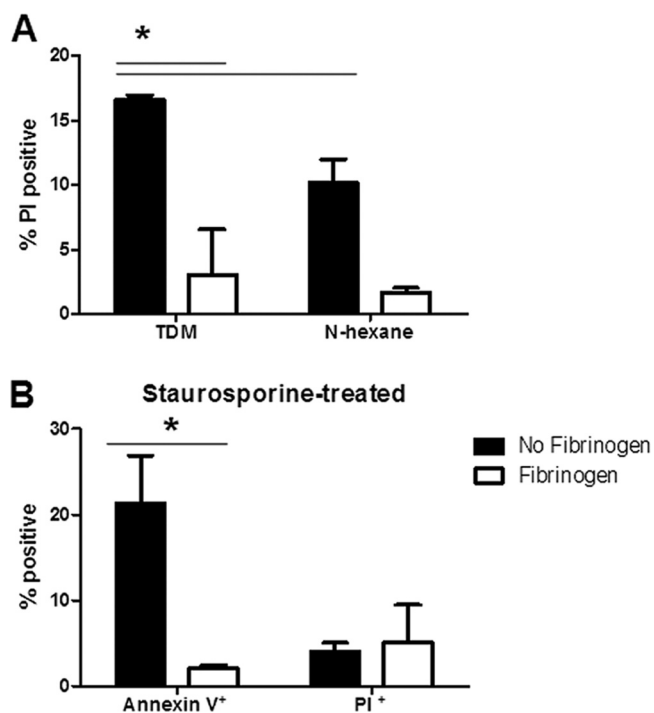
FIG. 4. Fibrinogen suppresses TDM-induced neutrophil necrosis *in vitro*. Bone marrow-derived neutrophils were purified and stimulated by TDM, vehicle control (*n*-hexane), or 60 µM staurosporine for 2 h in the presence or absence of 500 µg/ml fibrinogen and then stained using propidium iodide (PI) and annexin V to determine the percentage of the neutrophil population that is necrotic or apoptotic, respectively, by flow cytometry. (A) TDM induces a significantly higher percentage of PI-positive cells above that of the vehicle (*n*-hexane) control, and this percentage is significantly reduced in the presence of fibrinogen. (B) Staurosporine-induced neutrophil apoptosis, but not necrosis, also is significantly reduced in the presence of fibrinogen. Data from triplicate samples from a representative experiment are shown as means ± standard deviations, and asterisks indicate statistically significant differences ($P < 0.05$).
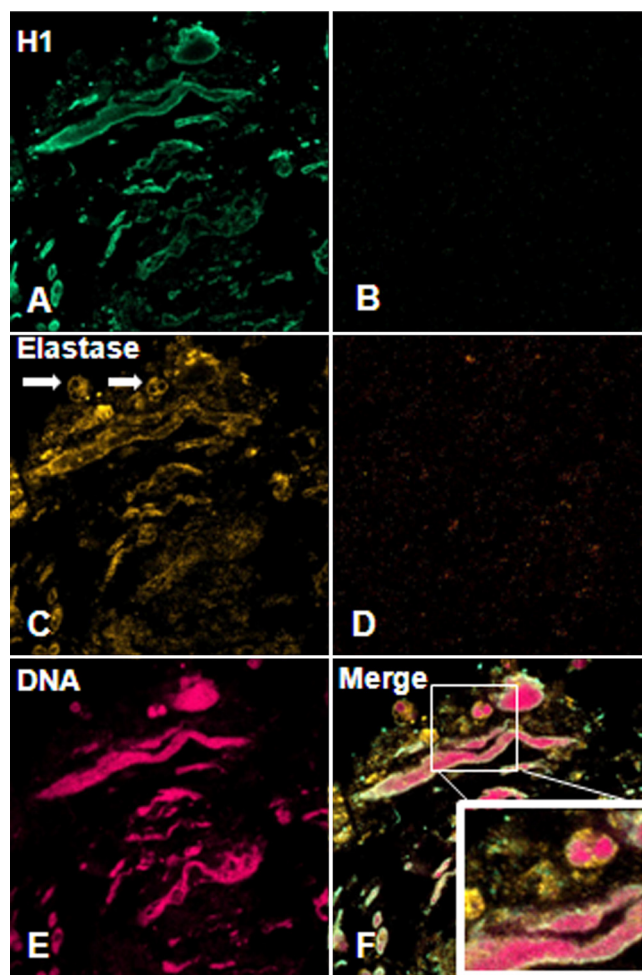

FIG. 5. TDM induces NETs in the absence of fibrinogen. Sections of 7-day-old TDM matrices from Fib KO mice were labeled using rabbit anti-human neutrophil elastase and mouse anti-human histone H1, followed by Alexa Fluor 555 goat anti-rabbit and Alexa Fluor 488 goat anti-mouse antibodies and the DNA stain Draq5, and then examined by confocal immunofluorescence microscopy. (A) Histone H1 is observed along the surface of the streaming DNA. (C) Neutrophil elastase is observed within intact neutrophils (arrows) as well as along the streaming neutrophil DNA. (E) Draq5 staining indicates that this streaming material is composed of DNA. (B and D) Negative control sections were stained only with secondary antibody for H1 and elastase, respectively.

responses to TDM nor the overall control of infection with *M. tuberculosis*.

DISCUSSION

The tuberculosis granuloma represents a complex dance between the bacillus and the host. Mycobacterial components stimulate a robust but organized leukocyte response that serves to contain the mycobacteria while not eradicating them completely, allowing the host and parasite to coexist for decades. However, some granulomas in some individuals progress to necrosis and caseation, facilitating the release of bacteria into the airways and, therefore, transmission. The factors that determine whether this progression occurs currently are unknown. TDM, a strong proinflammatory mycobacterial cell wall component, is postulated to play a dominant role in driving granuloma development and breakdown.

Fibrin(ogen) is a critical component of the acute inflammatory response and forms a scaffold along which leukocytes, endothelial cells, and fibroblasts could migrate in order to begin the repair process. Fibrin(ogen) has been described as a necessary cofactor for the toxic and proinflammatory activities of TDM (25). This would have predicted that Fib KO mice would mount a lesser inflammatory response to TDM. Interestingly, Fib KO mice showed exacerbated immunopathology, no reduction in either cell recruitment or proinflammatory cytokine response to TDM-coated particles, and no clear phenotype in intravenous or aerosol infection with *M. tuberculosis*. The response in Fib KO mice to TDM was more suppurative, which, while not appreciated by FACS analysis, clearly could be observed by histopathology. This discrepancy likely is due to the exclusion of dead (propidium iodide-positive) cells and debris in the FACS analysis. Slight kinetic differences were observed in the granulation tissue and neovascularization response to these matrices, processes that are well documented in the literature to rely on fibrinogen (5, 8, 33). This disorga-

TABLE 1. Absence of fibrinogen results in only a slight, transient decrease in liver bacterial burden on day 17 of infection with *M. tuberculosis*

Day	Group	Log_{10} CFU per organ[a]		
		Lung	Spleen	Liver
1	HET	1.58 ± 0.27		
8	HET	5.84 ± 0.17	5.00 ± 0.14	2.53 ± 0.27
	KO	5.70 ± 0.05	4.96 ± 0.19	2.48 ± 0.33
17	HET	6.03 ± 0.21	4.87 ± 0.35	3.89 ± 0.19
	KO	5.93 ± 0.14	4.99 ± 0.16	3.57 ± 0.05[b]
30	HET	5.49 ± 0.12	4.20 ± 0.17	4.28 ± 0.43
	KO	5.41 ± 0.06	4.3 ± 0.00	4.46 ± 0.73
60	HET	5.76 ± 0.08	4.30 ± 0.35	4.68 ± 0.19
	KO	5.71 ± 0.18	4.32 ± 0.28	4.83 ± 0.02

[a] Values are means $\pm$ standard deviations (4 mice per group) for *M. tuberculosis* CFU in organ homogenates from Fib HET or KO mice.
[b] Significantly different ($P < 0.05$) from the value for HET mice at 17 days of infection as calculated by Student's *t* test.

nization of granulation tissue in Fib KO mice may have allowed greater access to the matrices by neutrophils. These results suggest that perhaps fibrin(ogen) plays a more important regulatory role in the response to mycobacterial TDM than previously postulated, at least in the subcutis.

While our results show that fibrin(ogen) is not a required cofactor for TDM-induced inflammation or control of infection, we show that fibrin(ogen) plays a vital role in the initial containment of inflammation, as the TDM matrices splintered after intraperitoneal injection in Fib KO mice and subcutaneous matrices showed delayed capsule formation (Fig. 3E and data not shown). A factor to consider is that fibrin usually is present in greater amounts within the peritoneal cavity after infection or surgery due to decreased fibrinolytic activity, suggesting that there are differences in the role of fibrin(ogen) between different body compartments (37). It is interesting, however, that leukocytes, endothelial cells, and fibroblasts, while perhaps delayed to a degree, were not impaired in their migration toward the TDM-coated microspheres without fibrin present to provide a scaffold or chemokine/growth factor gradient. It is possible that the Matrigel fulfilled this role in our model, since while growth factor reduced, this embryonic stem cell mouse sarcoma-derived substance contains known growth factors, such as transforming growth factor-β, and potentially unknown components that may affect leukocyte recruitment and survival, even though fibrinogen was not detected by immunoblotting. It also is possible that no extracellular matrix components actually are needed in the Matrigel model; however, the current study cannot distinguish between these two possibilities. In an attempt to address this problem, we added exogenous fibrinogen to the TDM bead-containing matrix in Fib KO mice. While the added fibrinogen correlated with a return to the histological appearance of the capsule of the WT matrices, confirming that fibrinogen supports the generation of granulation tissue, it did not reduce recruited leukocyte death. This method of complementing fibrinogen may not allow for its proper availability for regulating the cytotoxic effects of TDM; therefore, other *in vivo* scaffold systems such as poly(lactic-co-glycolic) acid currently are being investigated in our laboratory as a replacement for Matrigel. Invariably, what occurs during *in vivo* infection is the most relevant data, and the result that

no phenotype is observed with both intravenous and aerosol infection clearly supports that fibrinogen is not required for immune responses to *M. tuberculosis*.

The leukocyte death that was a predominant feature of the TDM matrices in Fib KO mice also may be the result of reduced neovascularization. In this model, we could only qualitatively assess neovascularization, at necropsy and by histopathology. Whereas 4- and 7-day-old matrices from Fib KO mice seemed less vascularized grossly and histologically, by 12 days no differences were observed between Fib KO and WT mice. It is possible that this delay resulted in a reduced oxygen supply to the center of the Fib KO matrices, causing necrosis secondary to hypoxia. In this case, the cytotoxic effect of TDM in the absence of fibrinogen would be an indirect result of the delay in neovascularization. A direct cytotoxic effect of TDM on neutrophils, however, was shown *in vitro* (Fig. 4A). Furthermore, necrosis was not limited to the centers of the Fib KO matrices but occasionally was observed surrounding TDM beads at the periphery and also within WT matrices that were well vascularized (Fig. 1D). Matrix degradation in the presence of fibrinogen, as studied by *in situ* zymography, is due primarily to matrix metalloproteinase 9 activity (K. Sakamoto, unpublished results), and certainly neutrophil elastases may play a role (Fig. 5); however, the mechanism of TDM-induced necrosis in the absence of fibrinogen needs further study.

Fibrinogen also may enhance the survival of recruited leukocytes. Studies have shown that the binding of fibrinogen to the integrin receptor $\alpha_M\beta_2$/Mac-1 is critical for leukocyte function and regulates apoptosis in neutrophils (11, 38, 39). The immunohistochemical staining of TDM matrices from both Fib KO and WT mice, however, showed no activated caspase 3 staining, suggesting that leukocyte death in this case is primarily by necrosis. Furthermore, bone marrow-derived neutrophils stimulated with TDM *in vitro* showed a significantly higher percentage of necrotic, but not apoptotic, cells in the absence of fibrinogen (Fig. 4A). The histopathologic appearance of dead neutrophils, along with the colocalization of neutrophil histone H1, elastase, and DNA in these lesions, suggests that TDM induces the formation of NETs in the absence of fibrinogen (Fig. 1F and 5). Why greater leukocyte necrosis and NET formation are observed in the absence of fibrinogen, however, still is unclear. The study of TDM effects in mice with a targeted deletion of the $\alpha_M\beta_2$ binding motif within the fibrinogen γ chain may help to answer this question (11).

There are many events that occur in the tuberculosis granuloma, and it is thought that not all are productive for the containment or resolution of the infection. TDM is thought to be a virulence factor because it reproduces several symptoms of tuberculosis, namely, the excessive production of proinflammatory cytokines, cachexia, weight loss, and local necrosis (and in some cases, caseous necrosis in mice) (17). In other reports, we have demonstrated that although TDM triggers granulomagenic events, they often are excessive and unregulated compared to the responses elicited by intact bacilli (13). Notably, TDM elicits the excessive production of TNF-α and recruits large numbers of granulocytes, events associated with destructive tissue remodeling and toxicity in mice. The mechanisms that drive these pathological events are unknown. Our current findings indicate that fibrinogen regulates the response to TDM in at least two ways: (i) fibrinogen contributes to limiting

leukocyte necrosis, and (ii) fibrinogen contributes to the formation of granulation tissue that may serve to contain the response.

REFERENCES

1. **Altieri, D. C., J. H. Morrissey, and T. S. Edgington.** 1988. Adhesive receptor Mac-1 coordinates the activation of factor X on stimulated cells of monocytic and myeloid differentiation: an alternative initiation of the coagulation protease cascade. Proc. Natl. Acad. Sci. USA **85:**7462–7466.
2. **Axelrod, S., H. Oschkinat, J. Enders, B. Schlegel, V. Brinkmann, S. H. Kaufmann, A. Haas, and U. E. Schaible.** 2008. Delay of phagosome maturation by a mycobacterial lipid is reversed by nitric oxide. Cell. Microbiol. **10:**1530–1545.
3. **Bach, T. L., C. Barsigian, D. G. Chalupowicz, D. Busler, C. H. Yaen, D. S. Grant, and J. Martinez.** 1998. VE-cadherin mediates endothelial cell capillary tube formation in fibrin and collagen gels. Exp. Cell Res. **238:**324–334.
4. **Brinkmann, V., U. Reichard, C. Goosmann, B. Fauler, Y. Uhlemann, D. S. Weiss, Y. Weinrauch, and A. Zychlinsky.** 2004. Neutrophil extracellular traps kill bacteria. Science **303:**1532–1535.
5. **Brown, L. F., N. Lanir, J. McDonagh, K. Tognazzi, A. M. Dvorak, and H. F. Dvorak.** 1993. Fibroblast migration in fibrin gel matrices. Am. J. Pathol. **142:**273–283.
6. **Busuttil, S. J., V. A. Ploplis, F. J. Castellino, L. Tang, J. W. Eaton, and E. F. Plow.** 2004. A central role for plasminogen in the inflammatory response to biomaterials. J. Thromb. Haemost. **2:**1798–1805.
7. **Chalupowicz, D. G., Z. A. Chowdhury, T. L. Bach, C. Barsigian, and J. Martinez.** 1995. Fibrin II induces endothelial cell capillary tube formation. J. Cell Biol. **130:**207–215.
8. **Drew, A. F., H. Liu, J. M. Davidson, C. C. Daugherty, and J. L. Degen.** 2001. Wound-healing defects in mice lacking fibrinogen. Blood **97:**3691–3698.
9. **Drew, A. F., H. L. Tucker, H. Liu, D. P. Witte, J. L. Degen, and P. G. Tipping.** 2001. Crescentic glomerulonephritis is diminished in fibrinogen-deficient mice. Am. J. Physiol. **281:**F1157–1163.
10. **Dye, C., S. Scheele, P. Dolin, V. Pathania, and M. C. Raviglione.** 1999. Consensus statement. Global burden of tuberculosis: estimated incidence, prevalence, and mortality by country. WHO Global Surveillance and Monitoring Project. JAMA **282:**677–686.
11. **Flick, M. J., X. Du, D. P. Witte, M. Jirouskova, D. A. Soloviev, S. J. Busuttil, E. F. Plow, and J. L. Degen.** 2004. Leukocyte engagement of fibrin(ogen) via the integrin receptor alphaMbeta2/Mac-1 is critical for host inflammatory response in vivo. J. Clin. Investig. **113:**1596–1606.
12. **Frieden, T. R., T. R. Sterling, S. S. Munsiff, C. J. Watt, and C. Dye.** 2003. Tuberculosis. Lancet **362:**887–899.
13. **Geisel, R. E., K. Sakamoto, D. G. Russell, and E. R. Rhoades.** 2005. In vivo activity of released cell wall lipids of Mycobacterium bovis bacillus Calmette-Guerin is due principally to trehalose mycolates. J. Immunol. **174:**5007–5015.
14. **Hamaguchi, M., L. A. Bunce, L. A. Sporn, and C. W. Francis.** 1993. Spreading of platelets on fibrin is mediated by the amino terminus of the beta chain including peptide beta 15–42. Blood **81:**2348–2356.
15. **Hernandez-Pando, R., A. K. Arriaga, C. A. Panduro, E. H. Orozco, J. Larriva-Sahd, and V. Madrid-Marina.** 1998. The response of hepatic acute phase proteins during experimental pulmonary tuberculosis. Exp. Mol. Pathol. **65:**25–36.
16. **Herrick, S., O. Blanc-Brude, A. Gray, and G. Laurent.** 1999. Fibrinogen. Int. J. Biochem. Cell Biol. **31:**741–746.
17. **Hunter, R. L., M. Olsen, C. Jagannath, and J. K. Actor.** 2006. Trehalose 6,6′-dimycolate and lipid in the pathogenesis of caseating granulomas of tuberculosis in mice. Am. J. Pathol. **168:**1249–1261.
18. **Hunter, R. L., M. R. Olsen, C. Jagannath, and J. K. Actor.** 2006. Multiple roles of cord factor in the pathogenesis of primary, secondary, and cavitary tuberculosis, including a revised description of the pathology of secondary disease. Ann. Clin. Lab. Sci. **36:**371–386.
19. **Mogues, T., M. E. Goodrich, L. Ryan, R. LaCourse, and R. J. North.** 2001. The relative importance of T cell subsets in immunity and immunopathology of airborne Mycobacterium tuberculosis infection in mice. J. Exp. Med. **193:**271–280.
20. **Mosesson, M. W.** 2005. Fibrinogen and fibrin structure and functions. J. Thromb. Haemost. **3:**1894–1904.
21. **Mullarky, I. K., F. M. Szaba, K. N. Berggren, M. A. Parent, L. W. Kummer, W. Chen, L. L. Johnson, and S. T. Smiley.** 2005. Infection-stimulated fibrin deposition controls hemorrhage and limits hepatic bacterial growth during listeriosis. Infect. Immun. **73:**3888–3895.
22. **Odrljin, T. M., C. W. Francis, L. A. Sporn, L. A. Bunce, V. J. Marder, and P. J. Simpson-Haidaris.** 1996. Heparin-binding domain of fibrin mediates its binding to endothelial cells. Arterioscler. Thromb. Vasc. Biol. **16:**1544–1551.
23. **Palumbo, J. S., K. W. Kombrinck, A. F. Drew, T. S. Grimes, J. H. Kiser, J. L. Degen, and T. H. Bugge.** 2000. Fibrinogen is an important determinant of the metastatic potential of circulating tumor cells. Blood **96:**3302–3309.
24. **Ramos-Kichik, V., R. Mondragon-Flores, M. Mondragon-Castelan, S. Gonzalez-Pozos, S. Muniz-Hernandez, O. Rojas-Espinosa, R. Chacon-Salinas, S. Estrada-Parra, and I. Estrada-Garcia.** 2009. Neutrophil extracellular traps are induced by Mycobacterium tuberculosis. Tuberculosis (Edinburgh) **89:**29–37.
25. **Retzinger, G. S., S. C. Meredith, R. L. Hunter, K. Takayama, and F. J. Kezdy.** 1982. Identification of the physiologically active state of the mycobacterial glycolipid trehalose 6,6′-dimycolate and the role of fibrinogen in the biologic activities of trehalose 6,6′-dimycolate monolayers. J. Immunol. **129:**735–744.
26. **Retzinger, G. S., S. C. Meredith, K. Takayama, R. L. Hunter, and F. J. Kezdy.** 1981. The role of surface in the biological activities of trehalose 6,6′-dimycolate. Surface properties and development of a model system. J. Biol. Chem. **256:**8208–8216.
27. **Rhoades, E. R., R. E. Geisel, B. A. Butcher, S. McDonough, and D. G. Russell.** 2005. Cell wall lipids from Mycobacterium bovis BCG are inflammatory when inoculated within a gel matrix: characterization of a new model of the granulomatous response to mycobacterial components. Tuberculosis (Edinburgh) **85:**159–176.
28. **Riipi, L., and E. Carlson.** 1990. Tumor necrosis factor (TNF) is induced in mice by Candida albicans: role of TNF in fibrinogen increase. Infect. Immun. **58:**2750–2754.
29. **Roberts, A. A., C. A. Belisle, J. Turner, M. Gonzalez-Juarrero, and I. Orme.** 2002. Murine models of tuberculosis, p. 433–462. In S. H. Kaufmann and D. Kabelitz (ed.), Methods in microbiology. Academic Press, London, United Kingdom.
30. **Robson, S. C., N. W. White, I. Aronson, R. Woollgar, H. Goodman, and P. Jacobs.** 1996. Acute-phase response and the hypercoagulable state in pulmonary tuberculosis. Br. J. Haematol. **93:**943–949.
31. **Rubel, C., F. G., Dran, G. Bompadre, M. B., Isturiz, M. A., and M. S. Palermo.** 2001. Fibrinogen promotes neutrophil activation and delays apoptosis. J. Immunol. **166:**2002–2010.
32. **Russell, D. G.** 2007. Who puts the tubercle in tuberculosis? Nat. Rev. **5:**39–47.
33. **Sahni, A., and C. W. Francis.** 2000. Vascular endothelial growth factor binds to fibrinogen and fibrin and stimulates endothelial cell proliferation. Blood **96:**3772–3778.
34. **Sporn, L. A., L. A. Bunce, and C. W. Francis.** 1995. Cell proliferation on fibrin: modulation by fibrinopeptide cleavage. Blood **86:**1802–1810.
35. **Standeven, K. F., R. A. Ariens, and P. J. Grant.** 2005. The molecular physiology and pathology of fibrin structure/function. Blood Rev. **19:**275–288.
36. **Suh, T. T., K. Holmback, N. J. Jensen, C. C. Daugherty, K. Small, D. I. Simon, S. Potter, and J. L. Degen.** 1995. Resolution of spontaneous bleeding events but failure of pregnancy in fibrinogen-deficient mice. Genes Dev. **9:**2020–2033.
37. **van Goor, H., J. S. de Graaf, J. Grond, W. J. Sluiter, J. van der Meer, V. J. Bom, and R. P. Bleichrodt.** 1994. Fibrinolytic activity in the abdominal cavity of rats with faecal peritonitis. Br. J. Surg. **81:**1046–1049.
38. **Walzog, B., F. Jeblonski, A. Zakrzewicz, and P. Gaehtgens.** 1997. Beta2 integrins (CD11/CD18) promote apoptosis of human neutrophils. FASEB J. **11:**1177–1186.
39. **Whitlock, B. B., S. Gardai, V. Fadok, D. Bratton, and P. M. Henson.** 2000. Differential roles for alpha(M)beta(2) integrin clustering or activation in the control of apoptosis via regulation of akt and ERK survival mechanisms. J. Cell Biol. **151:**1305–1320.
40. **Wilberding, J. A., V. A. Ploplis, L. McLennan, Z. Liang, I. Cornelissen, M. Feldman, M. E. Deford, E. D. Rosen, and F. J. Castellino.** 2001. Development of pulmonary fibrosis in fibrinogen-deficient mice. Ann. N. Y. Acad. Sci. **936:**542–548.

Editor: R. P. Morrison